Joint Precoding and Spreading in the Forward Downlink of Multi Spot-Beam Satellite Communication System

Abdulkareem Karasuwa[1], Jonathan Rodriguez[2] and Ifiok Otung[3]
University of South Wales, Pontypridd, CF37 1DL, United Kingdom

High Throughput Satellite (HTS) systems exploting frequency reuse via multi spot-beam transmission is one of the key enablers for delivering high data-rate broadband services. However, such systems are prone to co-channel interference (CCI) and technological limitations surrounding the generation and deployment of small spot-beam sizes. Therefore, interference mitigation techniques (IMT) are employed to combat the effect of CCI and to improve system performance. In this context, we investigate linear and nonlinear precoding schemes as IMT mitigation tools on the forward downlink of a multi spot-beam satellite under practical operating conditions. The simulation results have shown a gain in system performance, where non-linear precoding techniques outperform their linear counterparts. An investigative study exploiting the joint application of spreading with the proposed precoding schemes is also reported

Nomenclature

B	=	feedback matrix
E_{tx}	=	transmit symbol energy
$E\{.\}$	=	Expected value operator
F	=	feedforward matrix
G	=	extra gain matrix
$G_{u,max}$	=	user-terminal maximum gain
$G_{i,j}$	=	interferer gain towards user-terminal
H	=	channel matrix
$h_{i,j}$	=	elements of channel matrix
L	=	lower triangular matrix
$L_{FS,u}$	=	user-terminal free-space loss
$L_{FS,j}$	=	interferer free-space loss
N_c	=	number of reuse colours
N_r	=	number of receive antennas
N_t	=	number of transmit antennas
n	=	AWGN vector
P_{ZF}	=	zero-forcing precoding matrix
P_{MMSE}	=	minimum-mean-squared-error precoding matrix
s	=	transmit signal vector
γ_p	=	precoding loss
τ_m	=	constellation extension constant
β_{ZF}	=	zero-forcing power scaling factor
β_{MMSE}	=	minimum-mean-squared-error power scaling factor
σ^2_n	=	variance of noise
σ^2_s	=	variance of original transmit symbols
σ^2_x	=	variance of precoded symbols
y	=	received signal vector

---

[1] Student, Mobile and Satellite Communicatons Group, abdulkareem.karasuwa@southwales.ac.uk, Student Member.
[2] Professor, Mobile and Satellite Communicatons Group, jonathan.rodriguez@southwales.ac.uk, Not a Member.
[3] Professor, Mobile and Satellite Communicatons Group, ifiok.otung@southwales.ac.uk, Not a Member.

I. Introduction

The convergence of digital wireless networks and the internet has opened up new opportunities to the consumer society in terms of providing access to multimedia content and internet services on the move. We are now entertaining new possibilities in terms of connected smart infrastructures, enhanced broadband connectivity, and the tactile internet, as part of the evolution towards 5th Generation (5G) systems. On the other hand, satellite communications has also evolved from traditional satellite phone and observation services towards portable satellite internet systems, providing coverage to users in extreme geographical . Clearly, the question that arises is whether the two telecommunications systems can coexist to provide an integrated solution, where 5G can harness the benefits of satellite systems towards enabling new use-casses such as smart oil rigs, or towards offloading traffic from the mobile network, among others. In this context, the 3GPP 5G consortia have already taken steps towards envisaging satellite services as part of the 5G roadmap, enabling fixed, mobile and satellite convergence that create the need for high throughput satellite (HTS) aimed at delivering capacity in the order of *terabit-per-second* (Tbps) to cope with the steadily-increasing user-demand.[1]

In this regard, satellite systems must offer large capacity, excellent availability and quality-of-service (QoS) in a cost-efficient way.[2] Possible means of realising these goals include, widening the useable bandwidth, strengthening the transmitted radio power, use of efficient transmission strategies and robust signal processing. Together, these techniques will ensure that the required capacity, system flexibility and efficiency can be achieved.

When addressing capacity-enhancement requirements in satellite systems, available options include operating in the higher frequency bands – where abundant bandwidth resources are available; and the use of multi spot-beam transmission strategy to implement frequency (and polarisation) reuse schemes – which increases in principle, the satellite's usable bandwidth. Furthermore, HTS systems use the Digital Video Broadcasting - 2nd Generation (DVB-S2) advanced air interface, which combines various modulation schemes including QPSK, 8-PSK, 16-APSK and 32-APSK, with several distinct code rates. This enables the capability to adaptively maintain reliable transmission under severe link impairment, by switching between appropriate MODCODs.[3]

An example of transition into the higher frequencies is the K_a-band (20/30 GHz),which is already intensively used and becoming increasingly congested. Hence, systems are currently moving towards the less-exploited segments of the spectrum, such as Q/V-band and W-band. However, this transition towards higher frequencies is challenging, but the *Eutelsat 65 West A* satellite launched in 2016 represents a first step in this direction operating on the Q/V-band, aproviding the basis for an initial learning curve for the deployment of future terabit-class satellites that could be operational by 2020.[4]

Although Satellite systems operating on the higher grequency bands can in hindsight provide greater capacity, nonetheless also come with inherent drawbacks due to the channel propagation characteristics. Systems operating at 10 GHz and above are adversely affected by atmospheric impairments that degrade the quality of the transmitted signal with consequent impact on link capacity; the most prominent factors affecting the link quality being the rain attenuation and hydrometeor (mainly ice and rain) depolarisation-induced interference.[5] In order to overcome these adverse atmospheric effects, *fade mitigation techniques* (FMT) are implemented to ensure uninterrupted service at the desired Quality of Service (QoS). However, some variation of FMT implementations have the potential to contribute to interference in satellite systems.[2,5] In addition to operating in the higher frequency bands to enhance capacity, an alternative approach is the frequency reuse approach using multi-beam antennas (MBA), so that the available spectrum resources are efficiently utilised leading to significant increase in system capacity.[1,6,7] However, the main drawback is the co-channel interference (CCI) prevalent between spot-beams reusing the same portion of the bandwidth, that leaads to so called limitless capacity multiplicity[8]. Hence, there is a clear need to address the CCI problem in order to achieve the desired capacity enhancement required for the envisioned terabit-class HTS systems is necessary.[6]

Operational HTS systems deploying MBA include Avanti's *Hylas-1* and *Hylas-2*, Eutelsat's *Ka-Sat*, Inmarsat's *Global Xpress*, *EchoStar 17* and *EchoStar 19*, and *ViaSat-1* and *ViaSat-2*. *ViaSat-1* is the highest-capacity satellite, that entered service in January 2012[4] and has offered up to 140 Gbps throughput; although, *ViaSat-2* was recently launched in June 2017, with a theoretical design throughput of 300 Gbps. A *ViaSat-3* is planned for launch beginning in 2020, constituting a system of three K_a-band satellites, each offering 1,000 Gbps.[9] Figure 1 shows the trend of HTS systems throughput over recent years.

With the impact of CCI on multi spot-beam systems being problematic and performance-limiting, the use of *interference mitigation techniques* (IMT) is therefore crucial. IMTs are broadly classified into two – transmitter-side (e.g. applicable to the forward-link) and receiver-side (e.g. applicable to the reverse-link) techniques. In the following, we will focus on the transmitters-side techniques, which are otherwise known as *precoding*. Here, the transmitter, with knowledge of the *channel state information* (CSI), is equipped with the capability to adapt to the channel interference (and hence, removes interference) on *a priori* basis. The prominent merit of precoding lies with the complexity, where the task of signal processing is performed at the transmitter, leading to simple, power-efficient and cheaper receive user-terminal.[10] Precoding implementations are classified as *linear* or *nonlinear*.

The linear precoding approach has moderate implementation complexity. However, it is affected by energy enhancement problem, which results in the precoded symbols' average energy being greater than the original transmitted symbols' average energy, that renders its performance inferior relative to the nonlinear approach.[11] In order to circumvent this deficiency, the nonlinear precoding employ a *modulo-arithmetic* operator. The *Tomlinson-Harashima precoding* (THP)[12,13] is a particular approach of nonlinear precoding which represents a compromise between system's performance and implementation complexity.[14,15,16]

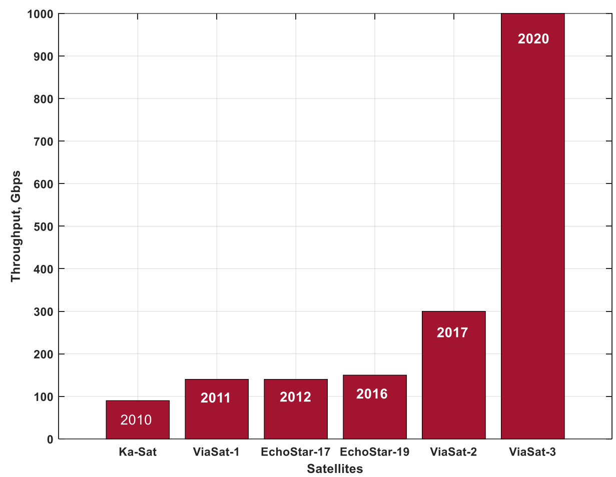

Figure 1. Growth of HTS systems throughput.

The satellite cellular systems for mobile and personal communications have exploited *code division multiple access* (CDMA) transmission as a potential candidate for implementing frequency reuse needed to increase capacity.[17] Important technical considerations for adopting spread-spectrum (SS) techniques over satellite, such as multiplexing, coding, and transmission of direct-sequence spread-spectrum (DS-SS) have already been established.[18] Hence, the evolution of the Universal Mobile Telecommunication System (UMTS) has spurred the satellite systems' CDMA component, leading to Inmarsat being the first to successfully GEO satellites providing UMTS-like services.[19]

In CDMA systems, original data symbols are encoded using binary signature symbols at the transmitter, producing a spread-spectrum signal, otherwise known as *chips*. The binary signature's rate is significantly higher than the data stream's rate. The receiver recovers the desired transmitted data symbols by correlating the incoming spread-spectrum signal with the appropriate user's signature.

Linear and nonlinear precoding techniques are also applicable to spread-spectrum based systems. A selection of linear precoding approaches are implemented for the downlink of direct-sequence CDMA (DS-CDMA) systems,[20] and a comparison of linear precoding with linear MUD in a downlink time division duplexing CDMA (TDD-CDMA) system is presented with results showing the precoding schemes outperforming the MUDs.[21] On the other hand, the performance of nonlinear precoding, the THP in particular, on CDMA systems are studied[22,23,24,25,26] and it is shown that the THP can also be combined with diversity techniques for frequency selective channels, with results showing the THP scheme outperformed their linear counterpart, as well as linear and nonlinear multiuser detection techniques (MUD) with comparable complexity.

In this paper, we investigated the performance of a selection of both linear and nonlinear precoding on the forward downlink of a multi spot-beam satellite system under varying system parameters and dimensioning. In particular, we incorporated spreading into a selection of precoding techniques and evaluated the system performance against baseline precoding techniques.

II. Multi Spot-beam Satellite System Channel Representation

Multi spot-beam satellite systems can be considered as typical *multiple-input-multiple-output* (MIMO) systems. Multiple antennas for wireless communication systems have gained remarkable attractiveness during the last few years, leading to the success of the 4G (4th Generation) LTE(long-term evolution) mobile system, and ushering in a new generation of MIMO antennas; the so called massive MIMO design that is playing a pivotal role in the 5G terrestrial network.[27] Multiple transmit and receive antennas are used to achieve *multiplexing gain* (enhancing bit-rate, leading to bandwidth efficiency), *diversity gain* (enhancing error performance, leading to power efficiency) and *array gain* (enhancing signal-to-noise-plus-interference ratio (SNIR), leading to interference reduction) in terrestrial wireless communication systems.[28] Figure 2 shows a variation of multiple antenna systems.

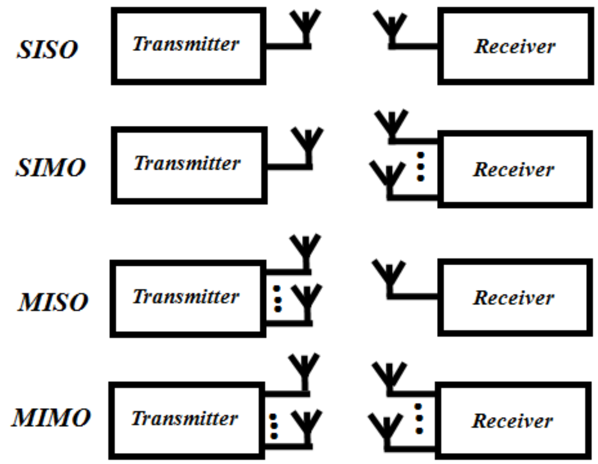

Figure 2. Multiple antenna systems representation.

The design of HTS system is based on multi spot-beam transmission strategy where the satellite antenna feeds (spot-beams) represents the transmit antenna elements, and the user-terminal(s)' antennas are considered as the elements of the receive antennas. In situations where there is cooperation between the receive user-terminals, such systems can be viewed as multi-user MIMO systems. Whereas, in situation where there is no cooperation between the receive user-terminals, the system is viewed as a *multiple-input-single-output* (MISO) systems. In general, the forward downlink (transmission from satellite to the user-terminals) of the multi spot-beam system can be regarded as a *broadcast channel* MIMO (MIMO-BC), and the return uplink (transmission from several user-terminals to the satellite antenna) is then considered to represent a *multiple access channel* MIMO (MIMO-MAC).[29] Figure 3 shows the multi spot-beam system and MIMO analogy.

Typically, a MIMO system can be described by the general basic vector relation:[30]

$$\boldsymbol{y} = \boldsymbol{Hs} + \boldsymbol{n} \tag{1}$$

where $\boldsymbol{H}$ represents the channel matrix and $\boldsymbol{s}$ is the transmitted signal column vector of size N_t, $\boldsymbol{s} = [s_1, s_2, s_3, ..., s_{\mathrm{Nt}}]^{\mathrm{T}}$. The received signal symbols $\boldsymbol{y}$ is a column vector of size N_r, $\boldsymbol{y} = [y_1, y_2, y_3, ..., y_{\mathrm{Nr}}]^{\mathrm{T}}$, $\boldsymbol{n}$ is additive white zero-mean complex Gaussian noise (AWGN) column vector of size N_r, $\boldsymbol{n} = [n_1, n_2, n_3, ..., n_{\mathrm{Nr}}]^{\mathrm{T}}$. It is worthy to note, that for a system with equal number of transmit and receive antennas (i.e. when $N_t = N_r$), $\boldsymbol{H}$ is a square matrix and therefore invertible directly.

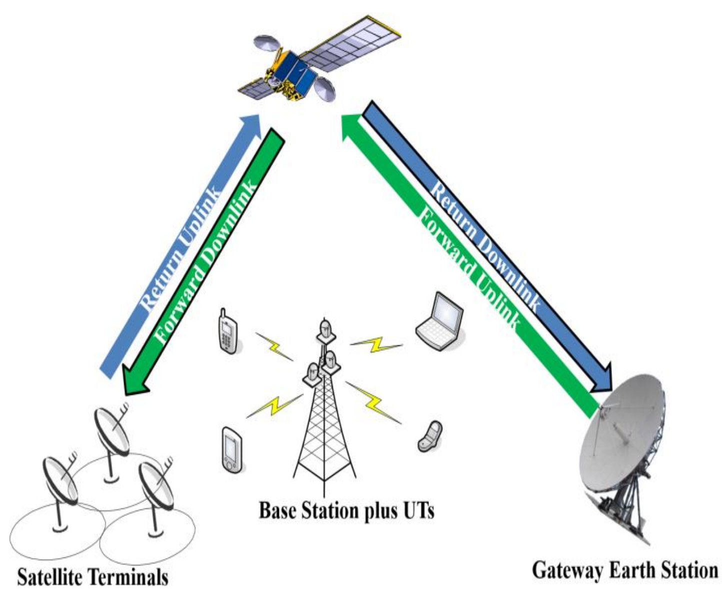

Figure 3. Multi spot-beam satellite system and analogy with MIMO system.

Considering a system where only one user exists in each of the spot-beams and no cooperation between them, if the number of spot-beams is N_{SB}, then, the transmit symbol vector $\boldsymbol{s}$ is of the dimension N_{SB} x 1, whereas the receive symbol vector $\boldsymbol{y}$ and the noise vector $\boldsymbol{n}$ are respectively of dimension N_r x 1. Therefore, the channel matrix $\boldsymbol{H}$ has dimension N_{SB} x N_{SB} ($N_t = N_r = N_{SB}$) and its h_{ij}

elements represents the complex impulse response between the j_{th} transmitter (spot-beam) and the i_{th} receiver user-terminal, where $i = 1, 2... N_r$ and $j = 1, 2... N_t$. For example, consider the i_{th} element of $\boldsymbol{y}$ which is given by:

$$\boldsymbol{y}_i = \sum_{j=1}^{N_{SB}} h_{ij}\boldsymbol{s}_j + \boldsymbol{n}_i \tag{2}$$

The channel is responsible for the interfering signal emanating from the spot-beams into each of the receiving user-terminals through the antenna side-lobe radiation pattern (or through the main lobe in severely interfered systems depending on the position of the interferer and the user within their respective spot-beams, and other factors, e.g. when the interferer(s)' power is greater than that of the user). Therefore, Eq. (2) can be rewritten as:

$$\boldsymbol{y}_i = h_{ii}\boldsymbol{s}_i + \sum_{j=1,\, j\neq i}^{N_{SB}} h_{ij}\boldsymbol{s}_j + \boldsymbol{n}_i \tag{3}$$

The significance of Eq. (3) is such that the wanted signal is scaled by the diagonal elements of the channel matrix h_{ii}, which translates into gain, and degraded by, in addition to AWGN channel, the summation of all off-diagonal elements of $\boldsymbol{H}$ ($h_{i\neq j}$). These off-diagonal elements account for the power emanating from the interfering spot-beams. The channel matrix $\boldsymbol{H}$, comprising of the absolute value of its coefficient and phase component is then represented by:

$$\boldsymbol{H} = \begin{bmatrix} |h_{1,1}|e^{j\theta_{1,1}} & |h_{1,2}|e^{j\theta_{1,2}} \cdots & |h_{1,N_t}|e^{j\theta_{1,N_t}} \\ |h_{2,1}|e^{j\theta_{2,1}} & |h_{2,2}|e^{j\theta_{2,2}} \cdots & |h_{2,N_t}|e^{j\theta_{1,N_t}} \\ \vdots & \vdots & \vdots \\ |h_{N_r,1}|e^{j\theta_{N_r,1}} & |h_{N_r,2}|e^{j\theta_{N_r,2}} \cdots & |h_{N_r,N_t}|e^{j\theta_{N_r,N_t}} \end{bmatrix} \tag{4}$$

And hence, the absolute values of the channel coefficient are determined using: [29]

$$|h_{i,j}| = \sqrt{\left(\frac{\mathrm{G}_{i,j}}{\mathrm{L}_{FS,j}}\right)\times\left(\frac{\mathrm{L}_{FS,u}}{\mathrm{G}_{ES,max}}\right)} \tag{5}$$

where $\mathrm{G}_{i,j}$ is the gain of the interferers towards the user-terminal, $\mathrm{L}_{FS,j}$ is the interferer(s)' free-space loss, $\mathrm{L}_{FS,u}$ is the user-terminal free-space loss and $\mathrm{G}_{u,max}$ is the user-termial maximum gain.

It should be remarked, that the interference power is influenced by factors such as the number of reuse colours, N_c; inter-beam isolation; location of the user and the interferers within the spot-beams; and the satellite antenna pattern which influences the power level in the side-lobes. For the case of a forward downlink, the interferers are the static co-channel spot-beams which are equidistant, and therefore the distance between each interferer and the user-terminal are the same. This results in the same path-loss and phase shift, and off-axis interfering antenna gain towards the user-terminal; which causes equal interference power contribution towards the user-terminal. Therefore, the CCI power is the sum of the all interference power from the co-channel spot-beams.

III. Precoding Techniques

The essence of *precoding* (both linear and nonlinear) is that the transmitter pre-processes the original data symbols such that interference is eliminated on *a priori* basis relying on the readiness of CSI at the transmitter, so that the signal at the receiver is undistorted.[31] For the CSI to be present at the transmitter, some means are employed to anticipate it. For instance, in a TDD system, the channel reciprocity between the downlink and uplink can be used to estimate the channel. However, in frequency division duplexing (FDD) systems, due to the lack reciprocity between the transmitter and receiver sides, the channel estimation is obtained via a feedback mechanism from the receiver.[30]

The use of linear precoding to curb the effect of CCI in the forward link of broadband multi spot-beam satellite system has been studied with results indicating potential increase in spectral efficiency culminating into system capacity enhancement.[32,33] On the other hand, a selection of nonlinear precoding approaches[14,16,34] have their implementations extended to a multi spot-beam satellite system in resulting in an improved systems performance.[35]

A. Linear Precoding Techniques

The two most prominent implementations of linear precoding are the *zero-forcing* (ZF-LP) and *minimum-mean-squared-error* (MMSE-LP).[14,36] The ZF-LP essentially inverts the transmission channel matrix $\boldsymbol{H}$ so that it can adapt the channel to the already known interference at the transmitter. The major drawback of the linear precoding, however, is that due to the channel inversion operation, the precoded symbol's average energy is increased with respect to energy of the original symbols (E_{tx}). The block diagram depicting linear precoding is shown in Fig. 4.

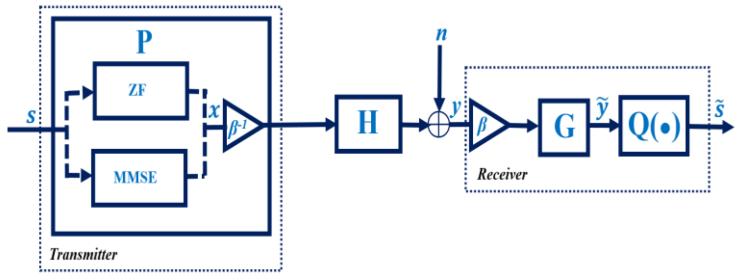

Figure 4. Block diagram of linear precoding system.

The original data symbol vector, $\boldsymbol{s}$, (QPSK, for example) is multiplied by the *precoding matrix*, $\boldsymbol{P}$, which may be designed based on ZF or MMSE strategy ($\boldsymbol{P}_{ZF}$ or $\boldsymbol{P}_{MMSE}$), with the sole purpose of pre-compensating for the effect of channel matrix $\boldsymbol{H}$. The presence of positive scalar factor β^{-1} at the transmitter is to meet the total transmitted power constraint after precoding, which is reversed at the receiver by β, and the receive signal is applied to an extra gain matrix, $\boldsymbol{G}$. Remark that, to ensure that the original data symbols' energy is equal to the precoded symbol energy, the following condition needs to satisfied:[37]

$$E\left\{\|\boldsymbol{x}\|^2\right\} = N_{SB}\sigma_x^2 = E\left\{\|\boldsymbol{s}\|^2\right\} = N_{SB}\sigma_s^2 \quad (6)$$

The variance of the transmitted precoded symbols is $E\left\{\boldsymbol{x}\boldsymbol{x}^H\right\} = \sigma_x^2\boldsymbol{I}$, and the precoded symbols vector, $\boldsymbol{x}$ can be obtained as:[30]

$$\boldsymbol{x} = \boldsymbol{P}\boldsymbol{s} \quad (7)$$

For a ZF precoding for a square invertible channel matrix $\boldsymbol{H}$, the matrix $\boldsymbol{P}_{ZF}$ can be expressed as:

$$\boldsymbol{P}_{ZF} = \beta_{ZF}^{-1}\boldsymbol{H}^{-1} \quad (8)$$

Whereas, for a non-invertible channel matrix, $\boldsymbol{P}_{ZF}$ can then be expressed as:

$$\boldsymbol{P}_{ZF} = \beta_{ZF}^{-1}\boldsymbol{H}^H(\boldsymbol{H}\boldsymbol{H}^H)^{-1} \quad (9)$$

and β_{ZF} is given as:

$$\beta_{ZF} = \sqrt{\frac{\mathrm{Tr}\left(\left(\boldsymbol{H}\boldsymbol{H}^H\right)^{-1}\sigma_x^2\right)}{E_{tx}}} \quad (10)$$

A variation of the ZF-LP method is the MMSE-LP, which takes into consideration the noise variance, σ_n^2, so as to improve system performance at low signal-to-noise (SNR) region, and σ_s^2 is variance of the transmitted symbol. In this case, the expressions for the precoding matrix $\boldsymbol{P}_{MMSE}$ and scaling constant β_{MMSE} are given by:[16]

$$\boldsymbol{P}_{\mathrm{MMSE}} = \frac{1}{\beta_{\mathrm{MMSE}}}\left(\boldsymbol{H}^{\mathrm{H}}\boldsymbol{H} + \frac{\sigma_n^2}{\sigma_s^2}\boldsymbol{I}\right)^{-1}\boldsymbol{H}^{\mathrm{H}} \tag{11}$$

$$\beta_{\mathrm{MMSE}} = \sqrt{\frac{\mathrm{Tr}\left(\left(\boldsymbol{H}^{\mathrm{H}}\boldsymbol{H} + \frac{\sigma_n^2}{\sigma_s^2}\boldsymbol{I}\right)^{-2}\boldsymbol{H}^{\mathrm{H}}\boldsymbol{H}\sigma_s^2\right)}{\mathrm{E}_{tx}}} \tag{12}$$

B. Nonlinear Precoding Techniques

The nonlinear precoding circumvents the energy enhancement problem associated with linear precoding. In nonlinear precoding, the average energy of the precoded symbols is nearly the same as the originally transmitted symbols (Eq. 6). The concept of nonlinearity in the transmit precoding can be traced back to Costa's DPC[38] which implies that, for channel interference that is known to the transmitter, the transmitted symbols can be pre-processed to adapt to the channel, as though there were no interference; thus, delivering a transmission rate equal to the channel's theoretical capacity boundary region.[39] However, the DPC scheme although being optimal in nature, has prohibitive complexity to be considered for practical implementation at both transmitter and receiver.[40, 41,42]

A relatively less complex and suboptimal implementation of the DPC is the THP.[43] The authors Tomlinson[12] and Harashima[13] both introduced relatively less-complex and suboptimal implementation of the DPC by integrating modulo-arithmetic operator into the precoding scheme. This introduces the nonlinearity that limits the transmit energy by ensuring that the symbols' amplitude is maintained within the boundaries of the original constellation. Figure 5 depicts nonlinear precoding system arrangement.

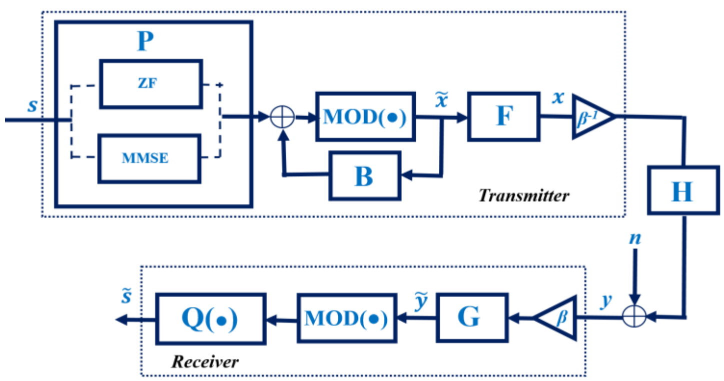

Figure 5. Block diagram of THP precoding system.

The matrices $\boldsymbol{B}$, $\boldsymbol{F}$, and $\boldsymbol{G}$ required for nonlinear precoding implementation can be calculated by performing a *QL-type decomposition* of the channel matrix $\boldsymbol{H}$:[11]

$$\boldsymbol{H} = \boldsymbol{F}^{H}\boldsymbol{L} = \boldsymbol{Q}^{H}\boldsymbol{L} \cong \boldsymbol{QL} \tag{13}$$

and hence, the matrices can be obtained by decomposing the channel matrix from Eq. (13):

$$\boldsymbol{H} = \boldsymbol{G}^{-1}\boldsymbol{B}\boldsymbol{F}^{H} \tag{14}$$

$$\boldsymbol{B} = \boldsymbol{GL} \tag{15}$$

$$\boldsymbol{G} = diag\left(l_{11},\ldots,l_{N_t,N_r}\right)^{-1} \tag{16}$$

where $\boldsymbol{F}$ is the unitary (i.e. $\boldsymbol{F}\boldsymbol{F}^H = \boldsymbol{I}$) feed-forward matrix and $\boldsymbol{L} = [l_{ij}]$ is a lower triangular matrix. $\boldsymbol{B}$ is a unit-diagonal lower triangular scaling matrix and $\boldsymbol{G}$ is a diagonal scaling matrix.

The modulo-adder MOD (•) shown in Fig. 6 works in this order: if the result of the summation is greater than M, then 2M is repeatedly subtracted until the result is less than M. Thus, when the result of the summation is less than –M, 2M is repeatedly added until the result is greater than or equal to –M.[11] For an *M-QAM* modulation, the modulo-operation MOD (•) is defined as:[15]

$$M\left(x_i\right) = x - \left\lfloor \frac{Re\left(s_i\right)}{\tau_m} + \frac{1}{2} \right\rfloor \tau_m - j\left\lfloor \frac{Im\left(s_i\right)}{\tau_m} + \frac{1}{2} \right\rfloor \tau_m \quad (17)$$

where τ_m is a constant for the periodic extension of the constellation that depends on the chosen modulation scheme. For QPSK, $\tau_m = 2\sqrt{2}$ and for square *M-QAM* $\tau_m = 2\sqrt{M}$.

However, as a result of the redistribution by the modulo-operation in Eq. (17), the precoded average transmit energy experiences a slight boost compared to the originally direct transmitted vector, $\boldsymbol{s}$. This is referred to as *precoding loss,* γ_p which depends on the value of M, and it is usually negligible for higher values of M. Theprecoding loss γ_p is obtained using:[11]

$$\gamma_p = \frac{M}{M - 1} \quad (18)$$

The original transmission symbols vector, $\boldsymbol{s}$, emanating from the modulation stage passes through a matrix $\boldsymbol{P}$ (of the order N_{SB} x N_{SB}).The modulo-operation is applied to the output $\boldsymbol{Ps}$ and then passes through a feedback loop via the lower triangular matrix $\boldsymbol{B}$. The matrix $\boldsymbol{B}$ premitigates the co-channel interference caused by earlier precoded symbols. The precoding operation is now applied to the output of the modulo-operation, $\tilde{x}$ successively, then $\tilde{\boldsymbol{x}}$ is passed through the feed-forward full matrix $\boldsymbol{F}$ yielding the precoded signal $\boldsymbol{x}$. The positive scalar factor β^{-1} is applied to the transmitted signal to comply with the transmit power requirements and it is reversed at the receiver via a corresponding factor β . The rescaled received signal $\boldsymbol{y}$, is then reapplied an extra gain which is represented by diagonal matrix $\boldsymbol{G}$. Finally, the modulo-operation is applied to the signal $\tilde{\boldsymbol{y}}$ and then the estimate $\tilde{\boldsymbol{s}}$ of the original signal is computed by the decision device $\boldsymbol{Q}$ (•).

C. Joint Precoding and Spreading

The application of both linear and nonlinear precoding to combat interference in multi spot-beam systems are justified by the benefits they offer. Aiming at further improvement in system performance, we investigate the application of spreading sequences with the precoding techniques. Spreading sequences are widely applied to multi-carrier CDMA (MC-CDMA) systems, where sub-carrier signals are spread by binary sequence codes in order to improve system performance. Figure 6 shows the proposed system. The precoded symbols vector $\boldsymbol{x}$ is hence multiplied by the spreading code (Walsh-Hadamard) **c,** of spreading gain G_s resulting in vector $\boldsymbol{d}$ (Eq. 19) to the transmitted via the channel. The precoding and spreading can be implemented separately.[24] However, these two processes can be implemented jointly motivated by well-known space-time precoding, where the spreading sequences are co-joined with the channel gain elements.[25]

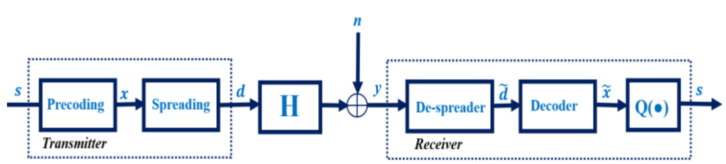

Figure 6. Proposed system for joint precoding and spreading implementation.

$$\boldsymbol{d} = \boldsymbol{C}^T \boldsymbol{Ps} \quad (19)$$

D. Simulation Results and Discussions

The results shown in Fig. 7 presents a comparison between linear and nonlinear ZF and MMSE precoding (QPSK system) schemes for N_c = 3 system. N_c = 3 represents a moderate interference effect which lies between N_c = 1 which is the severest, and N_c = 7 which is the least. The result shows that the nonprecoded system exhibits a floor (saturated) at lower SNR region indicating interference limitedness of the system. In the same vein, at lower SNR region, the nonprecoded system performs slightly better that the precoded systems, obviously due to inherent channel inversion and precoding loss associated with the precoding methods. Furthermore, the result shows that the MMSE approach outperformed the ZF in both the linear and nonlinear implementations. For a BER of 10^{-6}, for instance, for the linear system, the MMSE-LP shows a 3 dB gain over the ZF-LP approach, whereas, the MMSE-THP outperformed ZF-THP by 3.5 dB. Note that the result also shows that the ZF-THP outperformed the MMSE-LP by 0.5 dB.

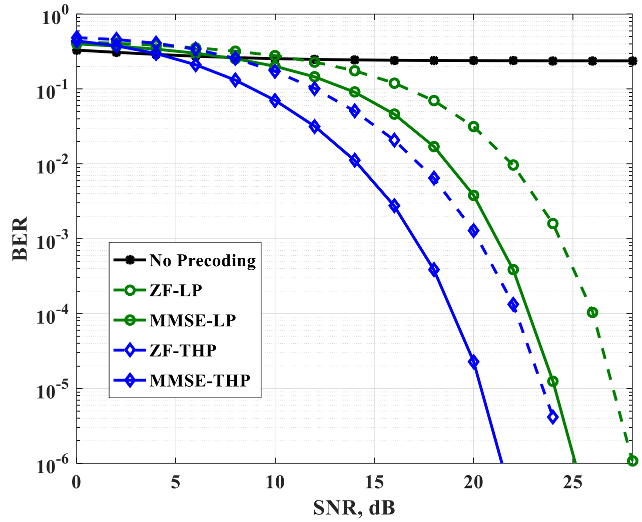

Figure 7. Linear and nonlinear implementation for a 7x7 system (QPSK, N_c = 3)

Figure 8 show the results of the MMSE-THP and ZF-THP implementations for different reuse numbers, N_c. The result indicated that systems with higher reuse number offer superior performance relative to those employing lower reuse number, for the two respective approaches. However, generally, MMSE-THP outperformed the ZF-THP. For a BER of 10^{-5}, for instance, the MMSE-THP outperformed ZF-THP in the order of 2.5 dB, 3.0 dB and 3.5 dB respectively for N_c = 1, N_c = 3, and N_c = 7 systems. On the other hand, considering the MMSE-THP systems alone, there is an improvement of 1 dB in system performance transitioning from N_c = 1 to N_c = 7. Whereas, a 0.5 dB improvement is observed for the ZF-THP increasing from N_c = 1 to N_c = 7. Overall, the results show that system performance depends on the number of reuse colours and the precoding approach employed for analyses.

Prelimenary results of the joint precoding and spreading for a ZF-LP system is presented in Fig. 9. The results show that the incorporation of spreading presents no significant difference in the lower SNR region. However, the ZF-LP system appeared to outperform the ZF-LP-plus-spreading system by about 1 dB as the SNR increases above 10 dB. This suggests that further investigation is required to fully analyse the system's performance under the this arrangement.

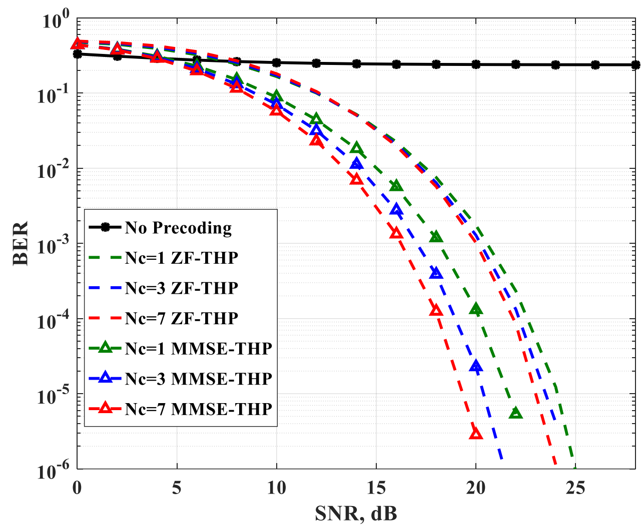

Figure 8. THP implementation for a 7x7 system (QPSK N_c = 1,3,7)

IV. Conclusion

In this paper, we have discussed the requirement of high-throughput-satellite (HTS) systems, and the problem of co-channel interference (CCI) on a multi spot-beam satelltile systems. Several precoding techniques used to mitigate the effects of CCI on system performance have been presented. Simulation results indicated that nonlinear precoding schemes outperformed their linear counterparts in all the systems considered. However, the integration of spreading with precoding over a multi spot-beam satellite system needs further investigation, as the preliminary results offer no improvement.

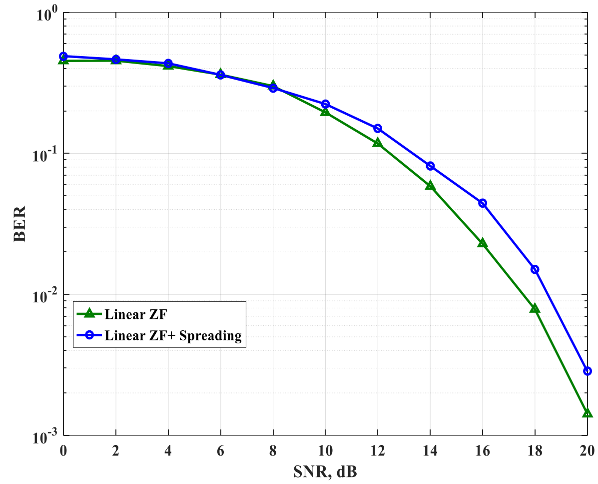

Figure 9. Linear ZF precoding plus spreading for a 7x7 system (QPSK, N_c = 1)

Acknowledgments

Abdulkareem Karasuwa would like to thank the Petroleum Technology Development Fund (PTDF), Abuja, Nigeria which has supported this work.

References

1. Kyrgiazos, A., Evans, B., Thompson, P., Mathiopoulos, P.T., and Papaharalabos. S. A., "Terabit/second Satellite System for European Broadband Access: A Feasibility Study". *International Journal of Satellite Communications and Networking* 2014; **32**(2): 63-92.
2. Castanet, L., Bolea-Almanac, A., and Bousquet, M., "Interference and Fade Mitigation Techniques for Ka and Q/V band Satellite Communication Systems". COST 272-280 Workshop. Noordwijk, The Netherlands; 2003.
3. ESTI. Digital Video Broadcasting (DVB); Second generation framing structure, channel coding and modulation systems for Broadcasting, Interactive Services, News Gathering and other broadband satellite applications (DVB-S2). ESTI EN 302 307 V131. France: European telecommunications Standards Institute; 2013.
4. Warwick, G., "*Frequency Shift - Higher frequencies promises to unlock greater capacity for faster internet service"* Aviation Week and Space Technology. 2017 6 - 19 March, 2017:58 - 9.
5. Panagopoulos, A. D., Arapoglou, P.M., and Cottis P.G., "Satellite Communications at KU, KA and V bands: Propagation Impairments and Mitigation Techniques". *Communications Surveys & Tutorials, IEEE* 2004; **6**(3): 2-14.
6. Gayrard J. D., Terabit Satellite: Myth or Reality? First International Conference on Advances in Satellite and Space Communications, SPACOMM 2009 20-25 July 2009; 2009. p. 1-6.
7. Thompson, P., Evans, B., Bousquet, M., Castenet, L., Mathiopoulos, T. "Concepts and Technologies for a Terabit/s Satellite: Supporting Future Broadband Services via Satellite". The Third International Conference on Advances in Satellite and Space Communications, SPACOMM 2011.
8. Lutz, E., "Co-channel Interference in High-Throughput Multibeam Satellite Systems". IEEE International Conference on Communications (ICC),; 2015 8-12 June 2015; 2015. p. 885-91.
9. Dubois, T., *Megabit for the Buck - Satelite operators urge OEMs to offer cheaper and more flexible capacity*. Aviation Week and Space Technology. 2017 6 - 19 March, 2017:60 - 1.
10. Joham, M., Utschick, W., and Nossek, J.A., "Linear Transmit Processing in MIMO Communications Systems". *IEEE Transactions on Signal Processing* 2005; **53**(8): 2700-12.
11. Fischer, R.F.H., *Precoding and Signal Shaping for Digital Transmission*. New York: John Wiley and Sons.; 2002.
12. Tomlinson, M., "New Automatic Equaliser Employing Modulo Arithmetic". *Electronics Letters* 1971; **7**(5): 138-9.
13. Harashima, H., Miyakawa, H., "Matched-Transmission Technique for Channels With Intersymbol Interference". *IEEE Transactions on Communications* 1972; **20**(4): 774-80.
14. Fischer, R.F.H., Windpassinger, C., Lampe, A., and Huber, J.B., "MIMO Precoding for Decentralized Receivers". Proceedings, IEEE International Symposium on Information Theory; 2002; 2002. p. 496.
15. Joham, M., Brehmer, J., Voulgarelis, A., and Utschick, W., "Multiuser Spatio-Temporal Tomlinson-Harashima Precoding for Frequency Selective Vector Channels". ITG Workshop on Smart Antennas; 2004 18-19 March 2004; 2004. p. 208-15.

16. Joham, M., "Optimization of Linear and Nonlinear Transmit Signal Processing" PhD Dissertation, Munich University of Technology; 2004.
17. Lutz, E., Werner, M., and Jahn, A., *Satellite Systems for Personal and Broadband Communications*. First ed. Berlin: Springer-Verlag; 2000.
18. Gaudenzi, R.D., Giannetti, F., and Luise, M., "Advances in Satellite CDMA Transmission for Mobile and Personal Communications". *Proceedings of the IEEE* 1996; **84**(1): 18-39.
19. Gaudenzi, R.D., Fanucci, L., Giannetti, F., Luise, M., and Rovini, M., "Satellite Mobile Communications Spread-Spectrum Receiver". *IEEE Aerospace and Electronic Systems Magazine* 2003; **18**(8): 23-30.
20. Jia, L., and Duel-Hallen, A., "Linear Multiuser Precoding with Transmit Antenna Diversity for DS/CDMA Systems". MILCOM 2005 - 2005 IEEE Military Communications Conference; 2005 17-20 Oct. 2005; 2005. p. 2823-9 Vol. 5.
21. Berenguer, I., Wang, X., Donaire, M., Reynolds, D., and Host-Madsen, A., "Linear Precoding Versus Linear Multiuser Detection in Downlink TDD-CDMA Systems". *IEEE Transactions on Wireless Communications* 2007; **6**(3): 780-6.
22. Jia, L., and Duel-Hallen, A., "Performance Analysis of Tomlinson-Harashima Multiuser Precoding in Multipath CDMA Channels". The 4G Mobile Forum Annual Conference; 2005.
23. Liu, J., and Duel-Hallen, A., "Tomlinson-Harashima Transmitter Precoding for Synchronous Multiuser Communications". Proc CISS'03; 2003; 2003.
24. Cosovic, I., Sand, S., and Raulefs, R., "A Non-linear Precoding Technique for Downlink MC-CDMA". 2005 IEEE 61st Vehicular Technology Conference; 2005 30 May-1 June 2005; 2005. p. 1711-5 Vol. 3.
25. Razavizadeh, S.M., Khandani, A.K., Vakili, V.T., and Tong, W., "Time-Space Precoding for Downlink Transmission in Multiple Antenna CDMA Systems". *IEEE Transactions on Vehicular Technology* 2007; **56**(5): 2590-602.
26. Liu, J., and Duel-Hallen, A., "Nonlinear Multiuser Precoding for Downlink DS-CDMA Systems over Multipath Fading Channels". Global Telecommunications Conference, 2004 GLOBECOM '04 IEEE; 2004 29 Nov.-3 Dec. 2004; 2004. p. 277-81 Vol.1.
27. Araújo, D.C., Maksymyuk, T., Almeida, ALFd., Maciel, T., Mota, J.C.M., and Jo, M., "Massive MIMO: Survey and Future Research Topics". *IET Communications,* 2016. http://digital-library.theiet.org/content/journals/10.1049/iet-com.2015.1091 (accessed.
28. Mietzner, J., Schober, R., Lampe, L., Gerstacker, W.H., and Hoeher, P.A., "Multiple-Antenna Techniques for Wireless Communications - A Comprehensive Literature Survey". *Communications Surveys & Tutorials, IEEE* 2009; **11**(2): 87-105.
29. Boussemart, V., Berioli, M., Rossetto, F., and Joham, M., "On the Achievable Rates for the Return-link of Multi-beam Satellite Systems using Successive Interference Cancellation". Military Communications Conference - MILCOM 2011; 2011. p. 217-23.
30. Cho, Y.S., Kim, J., Yang, Y.W., and Kang, C., *MIMO-OFDM Wireless Commuincations with MATLAB*. Singapore: John Wiley & Sons; 2010.
31. Sanguinetti, L., and Morelli, M., "Non-Linear Pre-Coding for Multiple-Antenna Multi-User Downlink Transmissions with Different QoS Requirements". *Wireless Communications, IEEE Transactions on* 2007; **6**(3): 852-6.
32. Cottatellucci, L., Debbah. M., Gallinaro, G., Mueller, R., Neri, M., and Rinaldo, R., "Interference Mitigation Techniques for Broadband Satellite Systems". *Proc 24th AIAA Int Commun Satell Systems Conf, ICSSC, San Diego CA* 2006; **1**: 1 - 13.
33. Devillers, B., and Perez-Neira, A., "Advanced Interference Mitigation Techniques for the Forward Link of Multi-beam Broadband Satellite Systems". Signals, Systems and Computers (ASILOMAR), 2011 Conference Record of the Forty Fifth Asilomar Conference on; 2011 6-9 Nov. 2011; 2011. p. 1810-4.
34. Joham, M., Brehmer, J., and Utschick, W., "MMSE Approaches to Multiuser Spatio-Temporal Tomlinson-Harashima Precoding". 5th International Conference on Source and Channel Coding (SCC '04). Erlange, Germany; 2004.
35. Diaz, M.A., Courville, N., Mosquera, C., Liva, G., and Corazza, G.E., "Non-Linear Interference Mitigation for Broadband Multimedia Satellite Systems". Satellite and Space Comm, 2007 IWSSC '07 International Workshop on; 2007 13-14 Sept. 2007; 2007. p. 61-5.
36. Windpassinger, C., Fischer, R.F.H., Vencel, T., and Huber, J.B., "Precoding in Multiantenna and Multiuser Communications". *Wireless Communications, IEEE Transactions on* 2004; **3**(4): 1305-16.
37. Fischer, R.F.H., Windpassinger ,C., Lampe, A., and Huber, J.B., "Tomlinson-Harashima Precoding in Space-Time Transmission for Low-rate Backward Channel". Broadband Communications, 2002 Access, Transmission, Networking 2002 International Zurich Seminar on; 2002 2002; 2002. p. 7-1-7-6.
38. Costa, M.H.M. "Writing on dirty paper" (Corresp.). *Information Theory, IEEE Transactions on* 1983; **29**(3): 439-41.
39. Weingarten, H., Steinberg, Y., and Shamai, S.S., "The Capacity Region of the Gaussian Multiple-Input Multiple-Output Broadcast Channel". *IEEE Transactions on Information Theory* 2006; **52**(9): 3936-64.
40. Zu, K., Lamare, R.Cd., Haardt, M., "Multi-Branch Tomlinson-Harashima Precoding Design for MU-MIMO Systems": Theory and Algorithms. *IEEE Transactions on Communications* 2014; **62**(3): 939-51.
41. Lee, J., and Jindal, N., "Dirty Paper Coding vs. Linear Precoding for MIMO Broadcast Channels". 2006 Fortieth Asilomar Conference on Signals, Systems and Computers; 2006 Oct. 29 2006-Nov. 1 2006; 2006. p. 779-83.
42. Poggioni, M., Berioli, M., and Banelli, P., "BER Performance of Multibeam Satellite Systems with Tomlinson-Harashima Precoding". 2009 IEEE International Conference on Communications; 2009 14-18 June 2009; 2009. p. 1-6.
43. Joham, M., Schmidt, D.A., Brehmer, J., and Utschick, W., "Finite-Length MMSE Tomlinson-Harashima Precoding for Frequency Selective Vector Channels". *IEEE Transactions on Signal Processing* 2007; **55**(6): 3073-88.